

## NUMERICAL SIMULATION OF AERODYNAMIC INSTABILITIES IN A MULTI-STAGE COMPRESSOR

**Fabien Wlassow**  
CERFACS, CFD Team  
31057 Toulouse Cedex01, France

**Nicolas Gourdain**  
CERFACS, CFD Team  
31057 Toulouse Cedex01, France

**Marc Montagnac**  
CERFACS, CFD Team  
31057 Toulouse Cedex01, France

### ABSTRACT

This paper aims to study the development of aerodynamic instabilities in a multistage compressor at near stall conditions. These phenomena are not fully understood because an unsteady approach is required to perform an effective simulation at a near stall operating point. The investigation methodology is based on a three-dimensional unsteady RANS simulation, considering the entire 3-stage compressor. Thus the low frequency that develops in the compressor can be captured. The flow unsteadiness are analysed by means of a modal approach. Rotor-stator interactions are characterised in two section of the compressor and axial waves associated with these interactions are observed. Finally a part span rotating stall is capture in the last stage.

### INTRODUCTION

With the development of CFD and high performance computers, the numerical simulation provides an alternative to experimental campaigns to improve the design process of turbomachines in terms of time and cost.

As the flow within a turbomachine is unsteady by nature an unsteady approach is necessary to obtain a better understanding of the aerodynamical behaviour, particularly at near surge operating points where unsteady effects have a strong influence on the engine performances. It is well known that the compressor operability is largely influenced by the tip clearance dimension [1] and that the tip leakage region exhibits usually the first signs of instabilities [2, 3]. Moreover the short axial distance between blades rows in modern compressors emphasises the flow unsteadiness and the rotor-stator interactions. Finally a better understanding of the aerodynamic instabilities that develop in modern turbomachines, especially in multistage

compressors, would enable to increase the compressor efficiency by means of a better surge margin management.

However since unsteady simulations were too expensive to be modelled in an industrial process, a steady mixing plane assumption [4] is often used. This approach consists in simulating only one blade passage using a steady RANS approach and applying circumferential averaging of the flow variables at the rotor-stator interfaces. Although the steady RANS approach allows significant reduction in computing cost, all the unsteady information is lost due to the averaging.

To overcome this lost of information several approaches have been proposed in order to reduce the computational cost of unsteady simulation. Among them, the Adamczyk flow model [5] is an alternative to unsteady RANS calculations. The simulation cost is lower than the cost of a full unsteady method but the unsteady stresses (i.e. the rotor-stator interactions) have to be modelled, adding a new difficulty not easy to overcome. Another method is the phase-lag assumption proposed by Erdos *et al* [6] to simulate rotor-stator interactions with the calculation of only one passage for each row. Nevertheless, this two methods use simplifying assumptions and thus they are not able to compute all unsteady effects and aerodynamic instabilities potentially present in a turbomachine. More recently, the development of spectral methods has proved to be a very efficient way to simulate periodic flows in a turbomachine stage and promising results have been obtained for multistage applications [7]. However, this technique has a validity domain limited to design conditions where frequencies and spatial wavelengths are known.

The computational power offered by massively parallel platforms enables to simulate the unsteady flow in an entire compressor with an unsteady RANS approach. As a consequence, no assumptions are made about the

frequencies of the instabilities present in flow and so a near stall operating point can be simulated. Few results have already been presented using this approach. Hathaway *et al* [8] have investigated the development of instabilities in an entire multistage compressor and Gourdain *et al* [9] have simulated a rotating stall in a single stage compressor. Van der Weide *et al* [10] have also shown the feasibility of the computation of a full multistage turbomachinery using a massively parallel platform.

Based on this state of the art, this paper focuses on the simulation of aerodynamic instabilities in a 3-stage compressor at a near stall operating point using a massively parallel platform and an unsteady RANS method. The main characteristics of the compressor test case and the numerical methodology, with a particular interest for the high performance computing strategy used, are presented in the first section. Then in the third section the unsteady behaviour is analysed in more details. The unsteady effects at two different rotor-stator interfaces are analysed using a spectral analysis. Finally, this study shows the feasibility of the simulation in the entire compressor at an operating point close to stall using massively parallel platforms. Moreover useful information about the aerodynamic instabilities that develop in a multistage compressor is provided.

## NOMENCLATURE

### Symbols

$L$  (m) distance from the hub

high-pressure compressor median-rear blocks of modern turbojet engines. The cylindrical outer casing diameter is 0.52 m. The nominal rotational speed is 11,543 rpm and the first rotor tip speed is  $313 \text{ m}\cdot\text{s}^{-1}$  (the corresponding Mach number is 0.92). The flow is transonic in the first stage and fully subsonic in the two last ones. The compressor is presented on Fig. 1 and the number of blades of each rotor and stator in Tab. 1. More details about the compressor can be found in Ottavy *et al* [11].

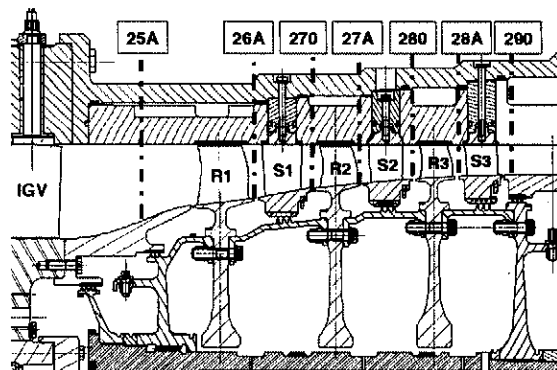


Fig. 1 Axial view of the CREATE compressor and measurement positions

used to compute the eddy viscosity and the flow is assumed to be fully turbulent since the Reynolds number based on the chord is around  $10^6$ .

In order to save CPU resources the IGV is not simulated but its influence is taken into account with an analytical model. For the same reason only one rotor chord of the inlet duct and of the outlet duct are represented. Finally, the secondary flow induced by the hub gap between rotating and non-rotating parts is not taken into account, mainly because blown and injected mass flows are not correctly known at these locations.

The 134.3 millions of nodes mesh (Fig. 2) used to discretise the entire compressor is based on a multi-block approach using an O-H strategy for each blade passage. The typical dimensions of a blade passage mesh are 85, 33 and 57 points, respectively in the axial, tangential and radial directions. An O-H mesh with 13 points in the radial direction is used to discretize the radial tip gap. To obtain a good balance between CPU cost and accuracy, a wall function approach is applied [17] with a fixed wall cell size corresponding to a mean normalized wall distance  $y^+$  of 20. It is well known that the wall function approach lacks of accuracy in the reverse flow areas, however the rotor-stator interactions studied in this paper are essentially piloted by inviscid phenomena. A sliding mesh condition with non matching points is applied at rotor-stator interface [18]. This method is conservative in the case of plane interfaces which is roughly the case here. A throttle condition coupled with a simplified radial equilibrium is used to model the outlet duct.

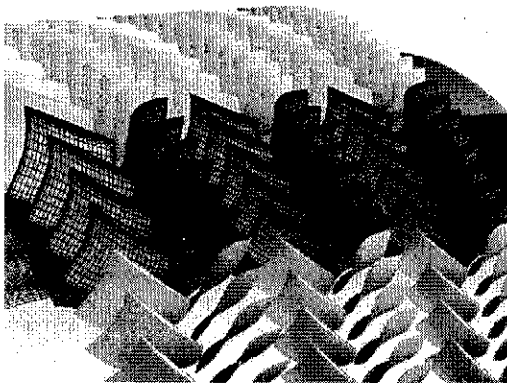


Fig. 2 Partial view of the mesh (1 on 2 points)

As a preliminary work, a periodic sector ( $1/16^{\text{th}}$ ) of the compressor has been studied in order to compute the operability range of the compressor and thus to determine a near surge operating point to perform the computation of the entire compressor. Then the unsteady computation of the entire compressor has been initialised with the solution

obtained with the reduced problem duplicated 16 times around the annulus. The unsteady computation of the entire compressor is performed with 4096 computing cores of a massively parallel platform IBM Blue Gene /P on which the performances of the *elsA* flow solver have been analysed for the simulation of the entire compressor at the design operating point [19].

### ANALYSIS OF THE UNSTEADY EFFECTS

The URANS simulation of the entire compressor has been carried out at a near surge operating point,  $\phi = 0.92$  (Fig. 3). After one and half rotation of the compressor a periodic state is reached, however the simulation was run for more than seven rotations in order to let possible low frequency instabilities develop. Figure 4 shows the entropy flowfield at  $h/H \sim 90\%$ . The wake interactions are well captured (Fig. 4). In addition a blockage area due to the tip leakage flow is visible near the second rotor tip (97.5%) and part span stall cells are visible in the third rotor. In fact, 32 cells are distributed alongside the azimuthal direction and their radial extension is about 10% of the compressor span (Fig. 5 – the axial velocity is normalized with the maximal axial velocity in this section). The mechanism responsible for this rotating instability is as follows. The tip leakage flow in the last rotor generates low axial momentum region in the rotor passage and behind the stator leading edge. These low axial momentum region interact with the stator wakes and create periodic boundary layer separation on the rotor suction side.

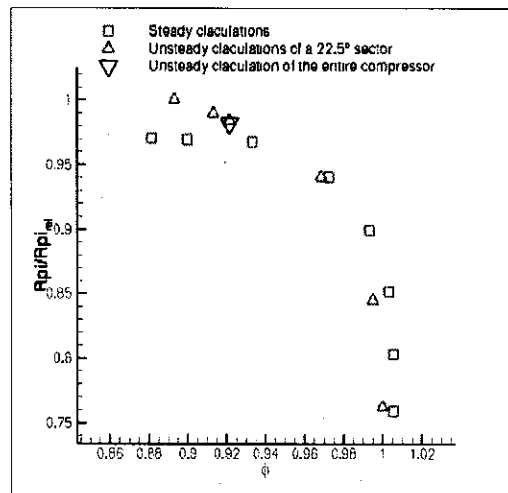


Fig. 3 Total-to-total pressure ratio

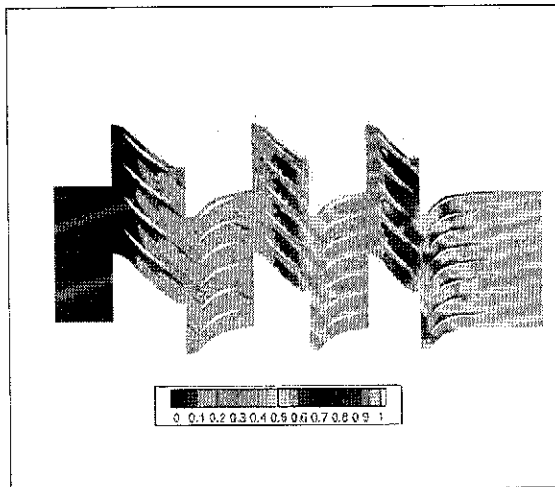


Fig. 4 Normalized entropy at  $h/H \sim 90\%$

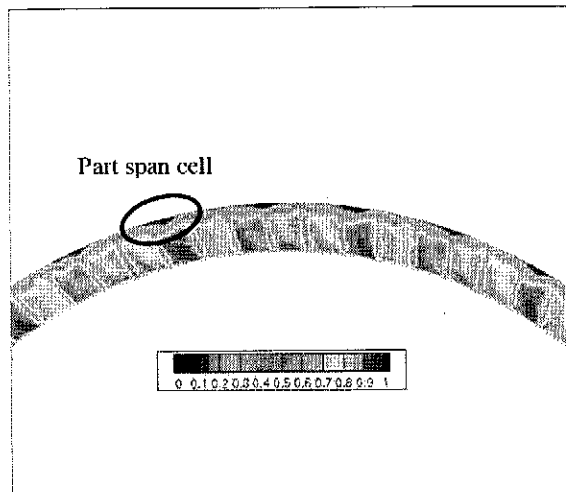


Fig. 5 Instantaneous axial velocity at section 28A

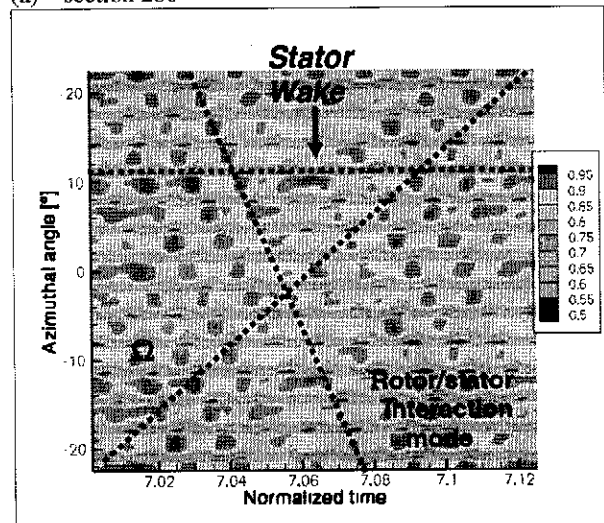
In order to analyze the unsteady effects that develop in the compressor and to assess the validity of the mechanism responsible for the rotating instability, the instantaneous flow variables are extracted during the computation at the rotor-stator interfaces 280 and 28A (Fig. 1).

**Investigation near the casing**

The investigations are firstly conducted at a fixed radial position near the casing ( $h/H \sim 95\%$ ). The instantaneous axial velocity at this radial position is represented with respect to the normalized time and the azimuthal direction at the section 280 and 28A (Fig. 6 (a) and (b)) the full domain is not represented for clarity reasons). The time period studied corresponds to a  $1/8^{\text{th}}$  of the seventh rotation. At the studied radial position, the flow field is influenced by different effects such as upstream

wakes, potential effects and tip leakage flow. Thus the analysis of these unsteady signals is challenging.

(a) – section 280



(b) – section 28A

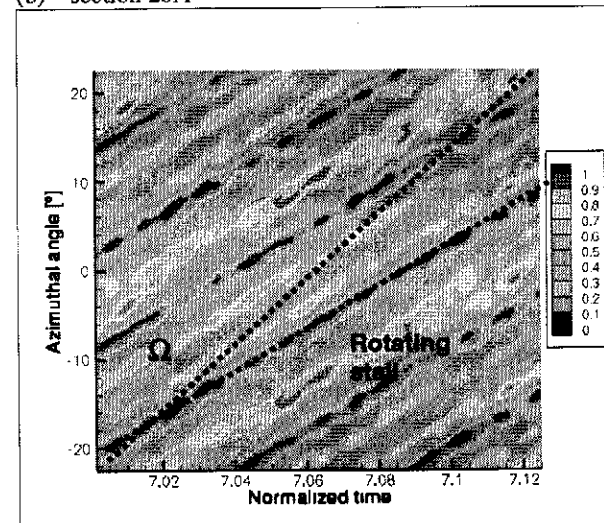


Fig. 6 Instantaneous axial velocity ( $h/H \sim 95\%$ ): (a) section 280, (b) section 28A

The analysis of the unsteadiness is based on the Tyler and Sofrin model [20]. The aerodynamic instabilities, such as rotor-stator interactions, are represented as a circumferential rotating wave defined with a spatial mode  $m$  and a rotating speed  $\Omega_m$ . The spatial mode is related to the spatial periodicity by  $m=2\pi/\lambda$  and corresponds to the repetition over the azimuthal direction of a specific pattern. This model can be used to predict rotor-stator interactions and more specifically the development of a spatial mode  $m$  (Eq. 1) and its rotating speed (Eq. 2). The sign of  $m$  indicates the direction of the rotation with respect to the rotor rotation. This model assumes that the rotational speed and the modal amplitude are constant.

$$m = nR + bS \quad (1)$$

$$\Omega_m = \frac{nR}{m} \Omega_R \quad (2)$$

In order to analyze the results from the simulation with this model, a Discrete Fourier Transform (DFT) is done considering the periodic spatial ( $\lambda=2\pi$ ) signal of the instantaneous axial velocity at successive temporal positions. To perform the DFT, the numerical signal is interpolated at equally spaced azimuthal positions with a linear method. Then the amplitudes and phases of the different spatial modes can be analysed. Recall that the phase corresponds in that case to the azimuthal position with respect to an arbitrary fixed position.

**Section 280:** Figure 7 shows the amplitude evolution of the spatial modes with respect to the normalized time. The analysis focuses on the spatial modes #80 and #112 as they have the greatest amplitudes. The spatial mode #112 is the strongest as section 280 is just downstream the 2<sup>nd</sup> stator which responsible for this spatial mode ( $n=0, b=1$  in Eq. 1). The spatial mode #80 is due to the 2<sup>nd</sup> and the 3<sup>rd</sup> rotor ( $n=1, b=0$  in Eq. 1). The phases and amplitudes of the spatial modes #80 and #112 are presented respectively in Fig. 9 and Fig. 10. Only 1/8<sup>th</sup> of a rotation is presented for clarity reasons. From the phase it is possible to retrieve the rotational speed of the mode as it is his derivative ( $\dot{\phi} = \Omega_m$ ). If  $p$  period of the phase of the mode  $m$  are observed during one rotor rotation, then  $\Omega_m = \frac{p}{m} \Omega_R$ . Thus from the numerical results we find that  $\Omega_{80} = \Omega_{rotor}$  and  $\Omega_{112} = 0$  which are the rotational speeds predicted by Eq. 2. However, although the Tyler and Sofrin model predicts constant amplitude for the spatial modes, a periodic evolution of the modes' amplitude is observed.

**Section 28A:** Figure 8 shows the amplitude evolution of the spatial modes with respect to the normalized time. The analysis focuses on the spatial modes #32 as it has the greatest amplitude at the section 28A. This mode results from the periodic interaction of the 2<sup>nd</sup> stator wakes ( $S2=112$ ) and the 3<sup>rd</sup> rotor tip leakage flow ( $R3=80$ ). The analysis of the phase (Fig. 11) shows that the rotational speed of this mode is a fraction of the rotational speed of the rotor, more exactly  $\Omega_{32} = 0.66\Omega$ . This mode is not in a synchronous with the rotor and, at this rotational speed, is not predicted by the Tyler and Sofrin model. This spatial mode corresponds to the rotating stall with 32 part span cells observed on the axial velocity flow field where the number of cells seems to be fixed by the rotor-stator interaction. Once again the time evolution of the amplitude is not constant.

Other spatial modes corresponding to rotor-stator interactions and predicted by the Tyler and Sofrin model are observed in the section 28A such as the modes #48, #64 and #96. However their phase and amplitude signals are harder to analyse as they are noised by the rotating stall. Actually the spatial mode #32, associated with the

rotating stall, and its harmonics are interacting with the rotor-stator interaction modes as the axial velocity fluctuations due to the rotating stall are superposing with those due to rotor-stator interactions. As these instabilities are not rotating at the same speed and have different amplitude fluctuations, the phase and amplitude signals of the spatial modes are made of the superposition of the different effects and thus no period can be easily defined.

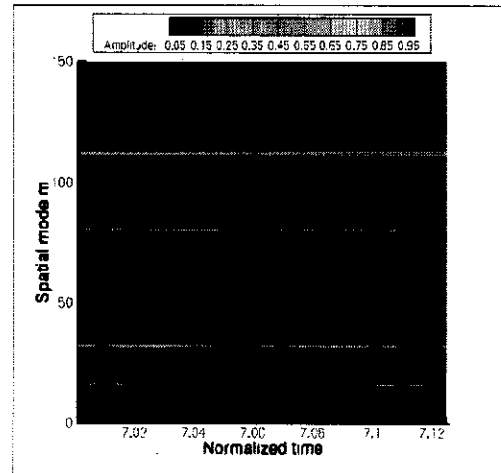


**Fig. 7 DFT of the instantaneous axial velocity signal – Section 280, h/H ~ 95%**

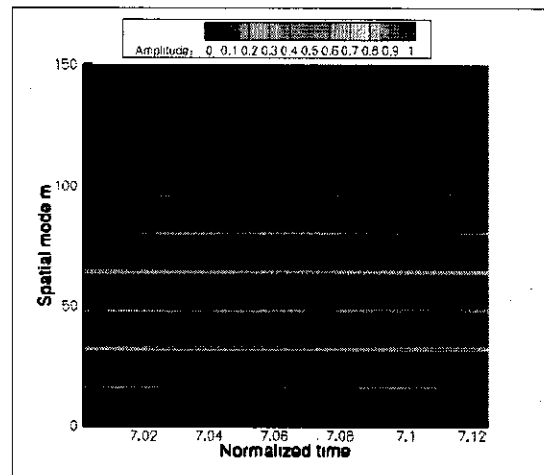
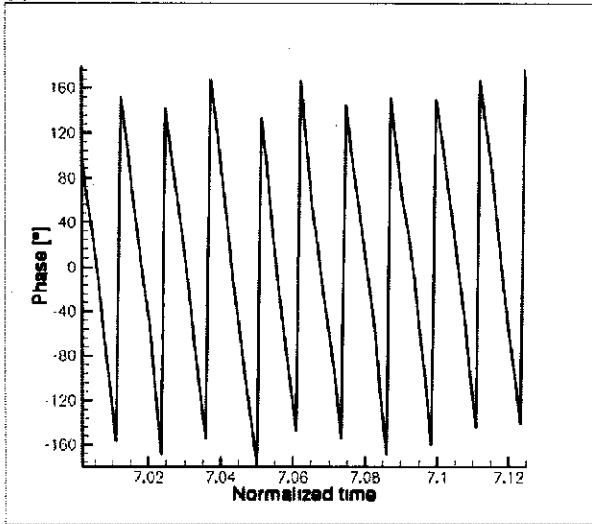


**Fig. 8 DFT of the instantaneous axial velocity signal – Section 28A, h/H ~ 95%**

(a) - Phase



(b) - Amplitude

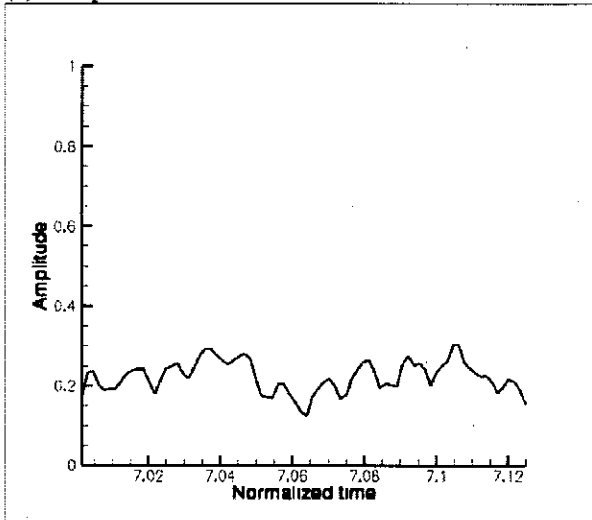
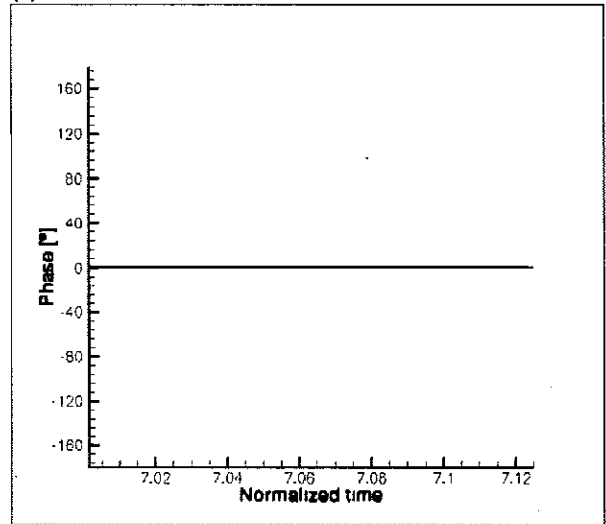


Fig. 9 Spatial mode 80 ( $h/H \sim 95\%$ , section 280):  
(a) Phase, (b) Amplitude

(a) - Phase



(b) - Amplitude

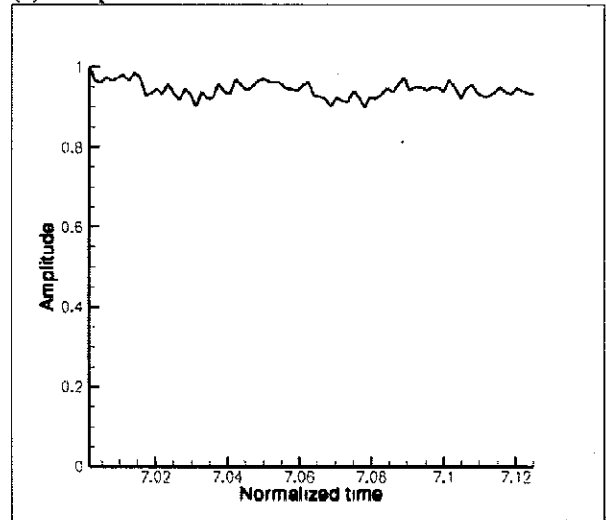
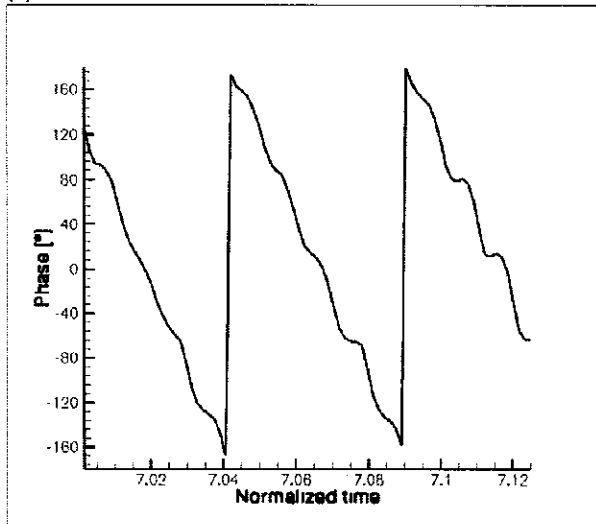


Fig. 10 Spatial mode 112 ( $h/H \sim 95\%$ , section 280):  
(a) Phase, (b) Amplitude

(a) - Phase



(b) - Amplitude

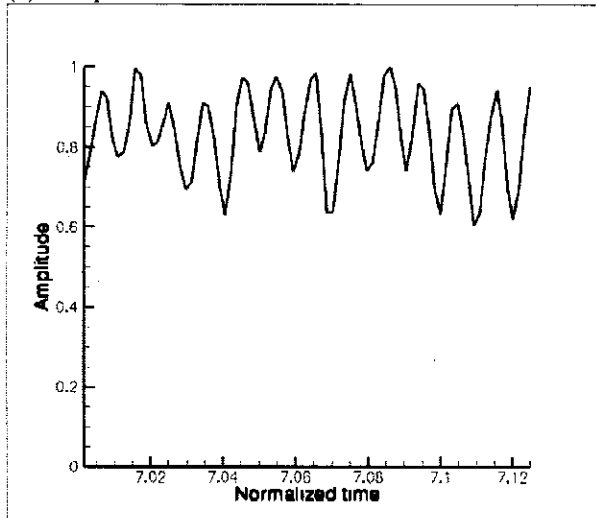


Fig. 11 Spatial mode 32 (h/H ~ 95%, section 28A):  
(a) Phase, (b) Amplitude

**One dimensional investigation:**

The previous investigation was only considering the effects at a fixed radial position near the casing. This way the time evolution of the spatial mode amplitudes can be due either to a radial or an axial transfer of axial velocity. To better understand this phenomenon the instantaneous axial velocity is now averaged along the radial direction. Thus the signals analysed correspond to a mean unsteady effects generated by the aerodynamic instabilities present at different radial positions. The radially averaged instantaneous axial velocity is also analysed by means of the Tyler and Sofrin model and a DFT.

**Section 280:** The strongest spatial modes of the radially averaged axial velocity signal is the modes #112 (Fig. 12) which is due to the influence of the 2<sup>nd</sup> stator. As it is a stationary mode, no amplitude or phase fluctuations are observed.

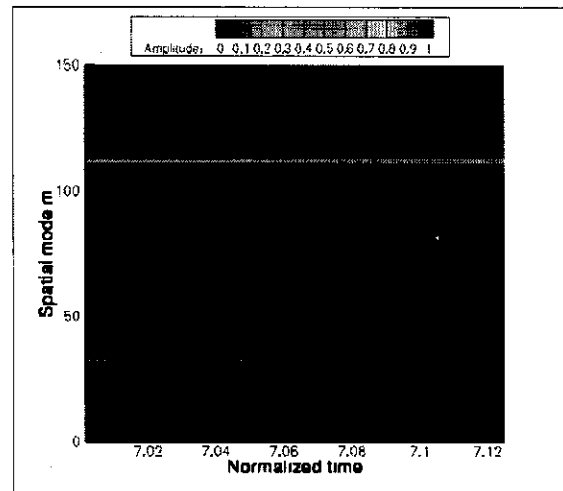


Fig. 12 DFT of the radially averaged axial velocity  
signal – Section 280

**Section 28A:** Even after the radial averaging, the spatial mode #32 is still strong. In fact the two strongest modes are the #32 and #80 (Fig. 13) which respectively correspond to the rotating stall and the influence of the rotor wakes. That means that the rotating stall has an influence on the whole blade span and not only near the casing. The amplitude signal of the mode #32 is periodic (Fig. 14) which shows the existence of an axial wave associated with this mode and thus with the rotating stall. The normalized frequency of this axial wave is  $f=96$ . Similarly, the periodic evolution of the amplitude of the mode #80 (Fig. 15) shows the existence of axial waves associated with this mode. The dominant normalized frequency of these waves are  $f=32$  and  $f=144$ . The intake and the plenum could play the role of resonators for these axial waves. However for the simulation the amounts of flow simulated upstream and downstream the compressor are not sufficient to allow these axial waves to develop and become as strong as it would be an actual engine.

**CONCLUSIONS**

This paper has presented the unsteady RANS simulation of an entire multistage compressor by means of a massively parallel platform. Because of the computational cost of the unsteady approach, a high performance computing strategy was used in order to perform the simulation with 4096 computational cores of a Blue Gene /P.

The flow unsteadiness has been analyzed by means of a modal approach. Thanks to this analysis, the rotor-stator interactions existing in the compressor have been identified and compared with the prediction of the Tyler and Sofrin theoretical model. This model predicts well the

mean features of the rotor-stator interactions even if it fails to predict the instantaneous evolution of the rotational speeds and amplitudes of the spatial modes. A better description of these phenomena could be achieved by taking into account the axial waves associated with these spatial modes. Finally a rotating stall in the last stage was successively captured by the simulation and characterized by the modal approach. Hence this rotating stall has 32 part span cells (covering 10% of the compressor span) rotating at 66% of the rotor rotational speed. An axial wave of frequency  $f=96$  is associated with this rotating stall. The mechanism responsible for this rotating instability is based on the interaction between the upstream stator wakes and the tip leakage flow in the rotor passage. Thus the rotor-stator interaction fixes the number of part span cells.

A perspective of this work will be the comparison of the present results with those of an experimental campaign. It will allow to qualify the accuracy of the unsteady simulation and especially to verify the existence of the part span rotating stall in the last stage. At the same time a simulation involving the intake and the plenum will be carried out in order to study more accurately the axial waves observed in this study.

**ACKNOWLEDGMENTS**

The authors are grateful to SNECMA for permission to publish results for the CREATE compressor. Special thanks to X. Ottavy for its collaborative work around the CREATE project and to the CERFACS - CFD Team and M. Gazaix (ONERA) for developing efficient numerical methods for the *elsA* software. The authors are also grateful to EDF for providing computational resources through a Blue Gene /P without which any unsteady calculation would have been possible.

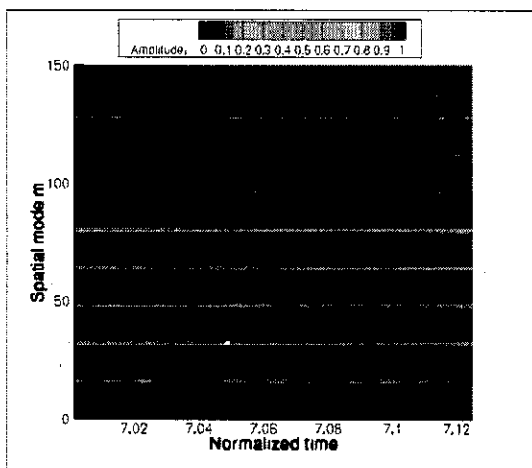
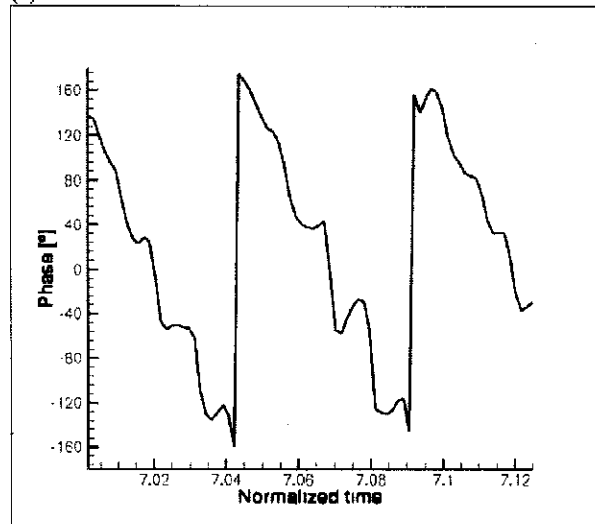


**Fig. 13 DFT of the radially averaged axial velocity signal – Section 28A**

**(a) - Phase**



**(b) - Amplitude**

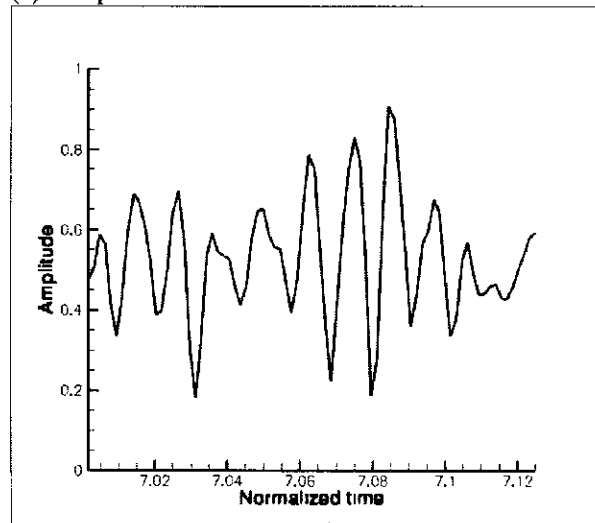
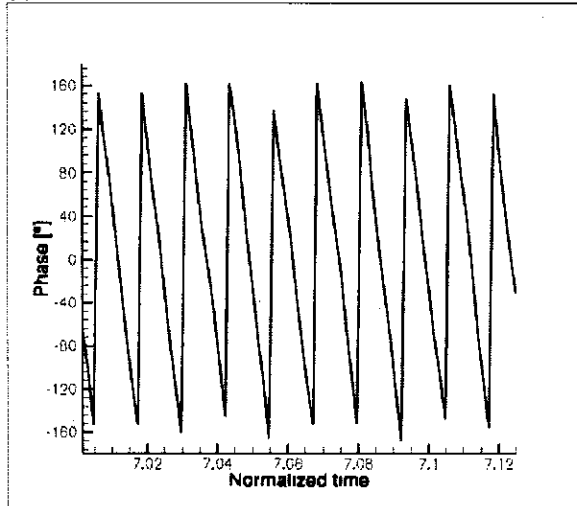
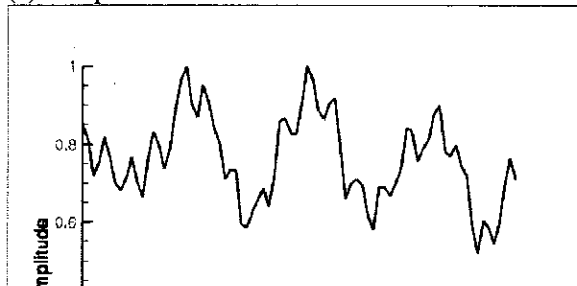


**Fig. 14 Spatial mode 32 (section 28A): (a) Phase, (b) Amplitude**

(a) - Phase



(b) - Amplitude



[4] Denton, J. D. and Singh, U.K., "Time Marching Methods for Turbomachinery Flow Calculations", VKI Lecture Series 1979-7, Von Karman Institute, Belgium, 1979

[5] Adamezyk, D., "Model Equation for Simulating Flows in Multistage Turbomachinery", Technical Memorandum 86869, NASA, USA, 1984

[6] Erdos, J. I., Alzner, E. and McNally, W., "Numerical Solution of Periodic Transonic Flow through a Fan Stage", AIAA J., Vol. 15, pp. 1559-1568, 1977

[7] Gopinath, A., Van Der Weide, E., Alonso, J. J., Jameson, A., Ekici, K. and Hall, K. C., "Three-Dimensional Unsteady Multi-Stage Turbomachinery Simulations using the Harmonic Balance Technique", 45<sup>th</sup> AIAA Aerospace Sciences Meeting and Exhibit, paper 2007-0892, Reno, USA, 2007

[8] Hathaway, M. D., Herrick, G., Chen, J. and Webster, R., "Time Accurate Unsteady Simulation of the Stall Inception Process in the Compression System of a US Army Helicopter Gas Turbine Engine", Proceedings of the DoD Users Group Conference, pp. 182-193, Washington, DC, USA, 2004

[9] Gourdain, N., Burguburu, S., Michon, G.-J., Ouayahya, N., Leboeuf, F., and Plot, S., "About the numerical simulation of unsteady flow in a turbomachinery stage"

[15] Yoon, S. and Jameson, A., "An LU-SSOR Scheme for the Euler and Navier-Stokes Equations", AIAA 25<sup>th</sup> Aerospace Sciences Meeting, paper 87-0600, Reno, USA, 1987

[16] Wilcox, D. C., "Reassessment of the Scale-Determining Equation for Advanced Turbulence Models", AIAA J., Vol. 26, pp. 1299-1310, 1988

[17] Goncalves, E. and Houdeville, R., "Reassessment of the wall functions approach for RANS computations", Aerospace Science and Technology, Vol. 5, pp. 1-14, 2005

[18] Fillola, G., Le Pape, M.-C. and Montagnac, M. "Numerical simulations around wing control surfaces", 24<sup>th</sup> International Congress of the Aeronautical Sciences ICAS, Yokohama, Japan, 2004

[19] Gourdain, N., Montagnac, M., Wlassow, F. and Gazaix, M., "High Performance Computing to Simulate Large Scale Industrial Flows in Multistage Compressors", to be published in Int. Journal of High Performance Computing

[20] Tyler, J. M. and Sofrin, T. G., "Axial Flow Compressor Noise Studies", SAE Transactions, Vol. 70, pp. 309-332, 1962